UCRL-18494

cy. 2

University of California

Ernest O. Lawrence Radiation Laboratory

RECEIVED
LAWRENCE
RADIATION LABORATORY

NOV 1 1968

LIBRARY AND
DOCUMENTS SECTION

K^+ MESON BRANCHING RATIO MEASUREMENT

M. E. Zeller, R. P. Haddock, J. A. Helland, J. Pahl, N. T. Dairiki,
R. L. Beck, K. M. Crowe, and M. T. Maung

September 26, 1968

TWO-WEEK LOAN COPY

This is a Library Circulating Copy which may be borrowed for two weeks. For a personal retention copy, call Tech. Info. Division, Ext. 5545

UCRL-18494 cy. 2

E

DISCLAIMER

This document was prepared as an account of work sponsored by the United States Government. While this document is believed to contain correct information, neither the United States Government nor any agency thereof, nor the Regents of the University of California, nor any of their employees, makes any warranty, express or implied, or assumes any legal responsibility for the accuracy, completeness, or usefulness of any information, apparatus, product, or process disclosed, or represents that its use would not infringe privately owned rights. Reference herein to any specific commercial product, process, or service by its trade name, trademark, manufacturer, or otherwise, does not necessarily constitute or imply its endorsement, recommendation, or favoring by the United States Government or any agency thereof, or the Regents of the University of California. The views and opinions of authors expressed herein do not necessarily state or reflect those of the United States Government or any agency thereof or the Regents of the University of California.

Submitted to Physical Review

UCRL-18494
Preprint

UNIVERSITY OF CALIFORNIA

Lawrence Radiation Laboratory
Berkeley, California

AEC Contract No. W-7405-eng-48

K^+ MESON BRANCHING RATIO MEASUREMENT

M. E. Zeller, R. P. Haddock, J. A. Helland, J. Pahl, N. T. Dairiki
R. L. Beck, K. M. Crowe, and M. T. Maung

September 26, 1968

K^+ MESON BRANCHING RATIO MEASUREMENT*

M. E. Zeller, R. P. Haddock, J. A. Helland†, and J. Pahl
University of California–Los Angeles
and
N. T. Dairiki, R. L. Beck‡, K. M. Crowe, and M. T. Maung**
Lawrence Radiation Laboratory
University of California
Berkeley, California

September 26, 1968

ABSTRACT

A measurement of the rates $K^+ \rightarrow \pi^0 + \pi^+$, $K^+ \rightarrow \mu^+ \pi^0 \nu$, and $K^+ \rightarrow e^+ + \pi^0 + \nu$ with respect to $K^+ \rightarrow \mu + \nu$ has been made by using a magnetic spectrometer and spark chambers. Both the range and momentum of the charged decay product are measured and compared with a Monte Carlo calculation. The decay in flight of the K^+ mesons and the scattering of pions into the apparatus are rejected by a decay-time requirement.

The results of the branching ratio measurement are $\Gamma(K_{\mu 2}) = (65.0 \pm 0.0)\%$, $\Gamma(K_{\pi 2}) = (19.8 \pm 1.1)\%$, $\Gamma(K_{\mu 3}) = (3.5 \pm 0.6)\%$, and $\Gamma(K_{e3}) = (4.4 \pm 0.4)\%$, on the assumptions $\Gamma(\tau) = (5.57 \pm 0.03)\%$ and $\Gamma(\tau') = (1.71 \pm 0.007)\%$.

I. INTRODUCTION

We report here the results of measurements of the branching ratios of the decay of the K^+ meson, in particular the relative rates of

$$K^+ \rightarrow \pi^+ + \pi^0 \quad (K_{\pi 2}),$$
$$K^+ \rightarrow \mu^+ + \nu + \pi^0 \quad (K_{\mu 3}),$$
and
$$K^+ \rightarrow e^+ + \nu + \pi^0 \quad (K_{e3})$$

with respect to the mode $K^+ \rightarrow \mu^+ + \nu$ $(K_{\mu 2})$. Table I and Fig. 1 show the results of previous measurements of these quantities.[1-15]

Prior to 1964, determinations of these branching ratios had been made by use of emulsions and heavy-liquid bubble chambers. Such measurements have two possible sources of systematic errors that limit the accuracy of the results: (a) K^+ decay in flight, which confuses the separation of the $K_{\mu 2}$ and $K_{\pi 2}$ modes from the other modes; (b) the energy dependence of the fiducial volume, which causes uncertainty in the number of detectable decays.

One of the objectives in the design of this experiment was to minimize these possible errors.

A second objective of the experiment was to obtain a more precise determination of the ratio $\Gamma(K_{\pi 2})/\Gamma(K_{\mu 2})$. There is presently no theoretical calculation of this ratio, but the previous experimental results are sufficiently scattered to warrant further investigation.

The hadron current describing the semileptonic three-body K decay involves two form factors, $f_+(q^2)$ and $f_-(q^2)$, which are scalar functions of the square of the four-momentum transferred to the leptons, q^2. Both the ratio of decay rates of these modes $\Gamma(K_{\mu 3})/\Gamma(K_{e3})$, and

the muon polarization can be expressed as functions of the ratio: $\xi(q^2) = f_-(q^2)/f_+(q^2)$. Present experimental evidence[16] indicates $\xi(q^2)$ is real; however, previous experiments yield widely varying results for the value of $\xi(q^2)$ as determined from branching ratios and measurements of $K_{\mu 3}$ muon polarization.[1-15, 17, 18] Figure 2 shows these results. A purpose of this experiment was to investigate this discrepancy.

It has been suggested that an underestimate of the momentum-transfer dependence of the form factors, $f_+(q^2)$ and $f_-(q^2)$, could be responsible for a misinterpretation of branching ratio measurements of the semileptonic modes.[18, 19] In calculating the effects of strong q^2 dependence we find it has little effect on the momentum spectra of the charged lepton.[20] Thus, allowing for a large variation of the form factors does not bring the value of ξ as determined by a measurement of $\Gamma(K_{\mu 3})/\Gamma(K_{e3})$ into agreement with that of the polarization measurement.

The form factors can be expanded in powers of q^2/m_π^2. If the dependence on q^2 is small only the first term need be retained:[21]

$$f_\pm(q^2) = f_\pm(0)\,[1 + \lambda_\pm(q^2/m_\pi^2)].$$

Previous experiments[22] have determined $\lambda_+ = 0.023 \pm 0.008$. As no precise measurement of λ_- has been made, we have assumed $\lambda_- = 0$.

In establishing the branching ratios, we have compared the data with theoretical predictions of the momentum spectra based on hypothesis of local leptonic coupling, muon electron universaility, and vector–axial-vector weak interactions.[23] The expression that is used

in relating ξ to the measured branching ratios of the semileptonic modes was obtained by Cabibbo:[24]

$$\Gamma(K_{\mu 3})/\Gamma(K_{e3}) = 0.6487 + 0.1045\, M_K^2 \lambda_+/M_\pi^2 + \mathrm{Re}[\xi(0)](0.1269 + 0.006\, M_K^2 \lambda_+/M_\pi^2) + |\xi(0)|^2 (0.0193 - 0.0053\, M_K^2 \lambda_+/M_\pi^2).$$

This equation was evaluated with $\lambda_+ = 0.023$ and $\xi(0) = f_-(q^2=0)/f_+(q^2=0)$.[25]

II. EXPERIMENTAL DETAILS

A. Beam

K^+ mesons were produced from protons in the external proton beam of the Bevatron impinging on a platinum target. The target was 6.5 cm along the proton beam, 0.62 cm wide, and 0.95 cm high. Figure 3 shows the transport system for the K^+ beam, 500-MeV/c ± 5%, from the production target to the K^+ stopping region. This system produced a K^+ image separated from the pions and protons by use of a separator with crossed electric and magnetic fields. It employed strong-focusing bending magnets (M2 and M3) to reduce the overall length of the flight path while retaining the focusing properties of a quadrupole system.

The momentum spread at the stopping target was reduced to ± 2% by means of a wedge-shaped carbon degrader placed at the first focus. The angular acceptance from the production target was 5 millisteradians, and the image size at the stopping target was 2.5 cm horizontally and 1.8 cm vertically. The vertical separation between K^+'s and protons was 6.1 cm, and between K^+'s and pions 2.1 cm. Approximately 3000 K^+ mesons were transmitted to the stopping target per Bevatron pulse

of 5×10^{11} protons incident on the production target, and of these, 800 were stopped.

B. Apparatus

Figure 4 shows a schematic drawing of the apparatus, including a typical K-decay particle trajectory. The directions and positions of an orbit were determined by twelve wire spark chambers placed at the entrance and exit of the spectrometer. The spectrometer was designed so that rays leaving the center of the target would focus on a plane approximately coincident with the F1 wire chamber independent of their initial angle.[26] The position along this focal plane of the image of such a point source is determined only by the momentum of the particles and the dispersion of the spectrometer, approximately 0.85 cm/(MeV/c). Another property of the spectrometer is that rays of different momentum leaving the center of the target along the optic axis all exit from the magnet parallel to one another. The momentum acceptance of the spectrometer is from 120 to 235 MeV/c.

Leaving the spectrometer, a particle continued on until it stopped in a spark chamber with twenty 0.635-cm aluminum plates (exit chamber). A wedge-shaped polyethylene degrader was placed between the exit of the spectrometer and the spark chamber so that the higher momentum muons from $K_{\mu 2}$ would stop in the exit chamber.

An event trigger was formed by a delayed coincidence between the stopping K^+ telescope, the decay telescope formed by S_{21} and S_{22}, and a pair of scintillation counters at the focal plane. The time between a stopping K^+ event and the subsequent decay product that passed through counter S_{21} and S_{22} was recorded with a time-to-height converter system,

and this information was used to reject events in which the K^+ decayed in flight.

Surrounding the K^+ stopping region was a set of three spark chambers with brass plates. These chambers were designed to detect the γ rays resulting from π^0 meson decay, and were not used in the aspect of the experiment herein reported.

C. Efficiency Measurements and Calibration

The efficiency of the focal-plane wire spark chambers was measured by extrapolating tracks observed in the exit spark chamber back to the focal plane. The ratio of the number of recorded wire chamber tracks to the total number of tracks then gave the efficiency as a function of position or momentum at the focal plane; the efficiency is shown in Fig. 5. The efficiency of the exit chamber was measured at the Berkeley 184-inch cyclotron and found to be $95 \pm 2\%$ efficient, independent of particle type or position in the chamber.

The spectrometer field was measured and fitted with simple polynomials to an accuracy of approximately 1%. This representation of the field was used in a computer program that simulated particle trajectories through the system. The accuracy of the orbit-tracking calculation was checked in two ways: (a) comparison with floating-wire measurements, and (b) comparison between prediction and actual position of the $K_{\mu 2}$ and $K_{\pi 2}$ momentum peaks. In the first method the program predicted wire trajectories to an accuracy of approximately 2 mm at any point along the wire. This uncertainty was included in the final analysis. The second check on the reliability of the program is discussed in the section describing the Monte Carlo calculation.

D. Data Collection and Reduction

A PDP-5 Digital Equipment Corp. on-line computer was used to monitor the data-taking process as well as to record the data on magnetic tape. Recorded data consisted of counter, wire chamber, and time-of-flight information for each event. In addition both a Vidicon system and a film camera were employed to digitize and record the spark positions of particle tracks in the exit spark chamber.

A data reduction program correlated the spark information into recognizable tracks, thinned the wire-chamber data, and merged the information on one tape with the counter data for each event. The wire chamber thinning involved the averaging of adjacent wire addresses and recording these averaged addresses as well as the number of wires averaged. The points at which the particle trajectory crossed the wire chambers were used to reconstruct the momentum and initial position and direction of each event. The particle range was calculated from the focal plane to the stopping point in the exit spark chamber.

As a measure of the quality of a particular event we calculated the distance between the actual position of the first spark in the exit spark chamber and the expected position (estimated by extrapolation from the focal plane wire chamber). Another quantity, χ_x^2, was used in assessing the event reconstruction. This was defined as the square of the difference (measured in units of the expected deviation) between the actual location of the sparks at the focal plane and the location predicted according to the entrance wire chamber addresses and the calculated momentum.

If one of the focal plane wire chambers failed to report, its address was constructed by an extrapolation from the wire chamber that did report to the first spark in the exit spark chamber. If neither focal plane chamber reported, the reconstruction was made by using the path of the track as observed in the exit chamber. All such reconstructions were noted on the output tape. For those events with more than one possible set of initial or final conditions, all possible combinations were formed and the set with the minimum χ_x^2 was chosen.

The resultant reconstruction for each event was then subject to a final reduction by a variety of requirements, which are discussed in Section IV.

III. MONTE CARLO CALCULATION

The procedure of the analysis was to compare the final data with distributions generated by a Monte Carlo calculation and determine the relative number of events for each mode with respect to the number for $K_{\mu 2}$. The routine was designed to simulate events and to analyze these events with the data-reduction programs. Decay events with initial momenta randomly generated from their respective theoretical momentum distributions were tracked by the orbit-tracking program through the system. The energy loss, straggling, and scattering were calculated for the hypothetical particle passing through the various pieces of material along the trajectory. For electrons, radiation and corrected ionization losses were included.[27-29]

The decay in flight and nuclear absorption of the pions were also simulated. In the case in which the mock pion had decayed (via $\pi \rightarrow \mu + \nu$)

in flight from the target to the exit spark chamber, the trajectory of the resultant muon was followed to the end of its range. Pion nuclear absorption was determined by using experimentally measured cross sections for nuclear interactions of pions in various materials, including large angle scattering and production of stars.[30,31] The wire chamber crossing positions, the counters that fired, and the positions of the first and last sparks in the exit spark chamber were generated, and this information was then processed by the data-analysis programs.

The scanning of the exit chamber included as primary tracks those decays which occurred within 10 deg of the initial particle direction. This bias was also included by calculation of the trajectory of the electron resulting from pion and muon decay at rest. The efficiency of the focal plane wire chambers as a function of momentum was included by folding the efficiency (see Fig. 5) into the momentum distributions for the different modes correcting for the fraction of reconstructed events.

Figure 6 shows four comparisons of the data with the Monte Carlo results. Plot I is a distribution of the length of $K_{\mu 2}$ muon tracks in the exit chamber. Plot II is the distribution of deviation of the first spark in the exit chamber from the projection using the focal plane wire chambers. Plots III and IV are distributions of particle initial position and angle respectively, as projected from entrance wire chamber addresses. The values of χ^2 divided by the number of degrees of freedom for these plots are 1.19, 1.99, 1.07, and 0.84 respectively. These particular distributions display the ability of the Monte Carlo calculation to simulate data. Plots I and II reflect the orbit tracking, while Plots III and IV indicate the acceptance by the spectrometer.

IV. DATA SAMPLE AND GATE REQUIREMENTS

The final data sample consists of 18 000 events in the momentum interval 120 to 240 MeV/c. The momentum distribution at the focal plane is compared with the Monte Carlo calculation in Fig. 7.

In Fig. 8 the data are shown as a two-dimensional plot of momentum vs difference between the observed range and the muon range for that momentum. In this plot muons appear in a horizontal band about $\Delta R = 0$, and pions appear in an approximately horizontal band about $\Delta R = -10.0$ g/cm^2; electrons have no definite range.

The data shown in Figs. 7 and 8 have been selected to satisfy various criteria that serve to remove background and ambiguous events. The selection requirements were chosen to minimize any biases that might depend on the mode of decay. The events generated by the Monte Carlo calculation were subject to the same selection requirements. These included a lower limit (approximately 15 nsec) on the decay time distribution,[32] to eliminate K^+ decay in flight and prompt pions scattering into the apparatus; an upper limit on χ_x^2 to minimize the number of events reconstructed from accidental wire addresses; and limits on the initial conditions of events to insure physically reasonable trajectories. Figure 9 shows the above distributions with their respective limits of acceptability.

V. FINAL ANALYSIS

A. Background Subtraction

There are three major sources of background: K^+ decay in flight, π^+ scattering out of the beam into the apparatus, and events coming from

sources other than the target. The decays in flight and the scatterings occur as prompt events with respect to the arrival of a trigger in the beam telescope and thus can be made negligible by adjustment of the lower limit on the decay time.

The remaining background was removed by a subtraction from the data. Comparison of the momentum spectrum of events originating from the target with that of events whose projected initial position is outside the target (see Fig. 9-I) shows that there are significantly more off-target events with momentum below the $K_{\mu 2}$ region. Explicitly, the ratio of events below 190 MeV/c to total events is $(14.8 \pm 1.1)\%$ for events originating inside the target volume $(31.0 \pm 2.5)\%$ for events originating outside. The larger fraction of low-momentum events results from an increase in material through which these particles pass, and the only such material is the γ-ray spark chambers positioned about the target. The K^+'s in the beam scatter out of the stopping region and stop in the plates of these chambers. The scattered K^+'s that decay from these plates are distributed nearly uniformly over the faces of the chambers, and some decay trajectories pass through the target volume. These events are indistinguishable from normal events in which the K stopped in the target; however, their momentum is reduced.

The range momentum distribution of the background was made by a Monte Carlo calculation assuming the scattered K^+'s to be uniformly distributed over the face of the chambers. The stopping positions in the brass were determined by using experimental range curves. The resultant range-momentum array (see Fig. 10) was normalized to the data by the fraction of background events under the peak of the initial position

distribution. A straight-line fit to the data outside the peak of Fig. 9-I was made. The number of events under this line that met the selection criteria was then used as the number of background events. The normalized background was subtracted from the data range-momentum plot.

B. Method

The branching ratio was finally determined by an analysis of the two-dimensional range-momentum scattergrams. These scattergrams were divided into regions or cells as shown in Fig. 8. This cell structure was chosen so that the majority of events could be classified as follows:

Cells (1, 1) and (1, 2) :	K_{e3} electrons;
Cell (3, 2) :	$K_{\mu 2}$ muons;
Cells (2, 1) and (2, 2) :	$K_{\mu 3}$ muons;
Cell (3, 1) :	$K_{\pi 2}$ pions;
Cells (2, 3) and (2, 4) :	$K_{\pi 2}$ muons from decay in flight and at rest, background from $K_{\mu 2}$ muons originating from within the plates of the brass spark chambers, and $K_{\mu 3}$ muons.

The τ and τ' modes of decay ($K^+ \rightarrow \pi^+\pi^-\pi^+$ and $K^+ \rightarrow \pi^+\pi^0\pi^0$) were excluded from the system due to insufficient range of the decay pions. To determine the relative branching ratios, $R_i = \Gamma_i/\Gamma(K_{\mu 2})$, with $i = K_{\pi 2}, K_{\mu 3}, K_{e3}$, a χ^2 function was constructed comparing the calculated and experimental data distributions on a cell-by-cell basis, and the χ^2 was minimized.[34] The uncertainties included in the

formation of the χ^2 function were those due to statistical uncertainties in the data and the Monte Carlo calculation, and the uncertainty in the focal plane wire chamber efficiency. In addition, instrumental uncertainties and possible systematic errors, presented in Table II, were added to the errors resulting from the χ^2 minimization routine.

C. Results

The range-momentum scatter plot for the final data sample is shown in Fig. 8 along with the division into bins. The calculated distributions for the four modes measured in this experiment are shown in Figs. 11 through 14. The background calculation is shown in Fig. 10. Table III shows the data array after background subtraction; the input to the χ^2 program for each mode, normalized and corrected for chamber inefficiencies; and the resulting composite array from the χ^2 minimization. The branching ratios calculated as relative rates normalized to the $K_{\mu 2}$ cell are

$$K_{\mu 2} = 0.997 \pm 0.015,$$
$$K_{\pi 2} = 0.304 \pm 0.017,$$
$$K_{\mu 3} = 0.054 \pm 0.009,$$
$$K_{e3} = 0.069 \pm 0.006.$$

The errors include statistical and systematic uncertainties as shown in Table II.

The reason the $K_{\mu 2}$ is not identically 1.000 is that a small amount of $K_{\mu 2}$ muons extend beyond the (3, 2) cell (see Table III). The actual normalization is to this cell, and the $K_{\mu 2}$ ratio is then evaluated along with the other branching ratios.

When one uses the accepted branching ratios for the three-pion modes, $\tau' = (1.71 \pm 0.07)\%$ and $\tau = (5.57 \pm 0.03)\%$[35] the branching ratios become

$$K_{\mu 2} = (65.0 \pm 0.9)\%,$$
$$K_{\pi 2} = (19.8 \pm 1.1)\%,$$
$$K_{\mu 3} = (\ 3.5 \pm 0.6)\%,$$
$$K_{e3} = (\ 4.4 \pm 0.4)\%.$$

Comparison of the composite range-momentum plot for the Monte Carlo calculation with the data array, using the above branching ratios, yields a χ^2 of 8.77 for six degrees of freedom.

From the above one has

$$\Gamma(K_{\mu 3})/\Gamma(K_{e3}) = 0.81 \pm 0.13,$$

which gives the form-factor ratio

$$\xi(0) = 0.91 \pm 0.82,$$

assuming $\lambda_+ = 0.023$ and $\lambda_- = 0.0$.

The momentum distribution of the $K_{\mu 3}$ mode was generated for both $\xi(q^2) = 0$ and $\xi(q^2) = 1.0$. These two spectra were compared with the data and both yielded the same value of $\Gamma(K_{\mu 3}) / \Gamma(K_{e3})$ to within the statistical significance of the experiment.

The result of the measurement of the $K_{\mu 2}/K_{\pi 2}$ ratio is

$$\Gamma(K_{\mu 2})/\Gamma(K_{\pi 2}) = 3.28 \pm 0.18.$$

D. Conclusion

As seen in Fig. 1, our results are in general agreement with previous measurements; in particular, we show general agreement with the other previous spectrometer measurements.[11, 14, 15] In view of the fact that our analysis was significantly different from previous methods and that the experimental apparatus was also different, the possible systematic errors of our results are, for the most part, different from previous branching-ratio determinations. That we do have an independent measurement and yet are also in disagreement with the polarization measurements of the parameter ξ indicates that the discrepancy is most likely not due to systematic errors in the branching-ratio measurements.

In Section I the possibility that the discrepancy between the measurement of ξ by different methods is due to a large momentum-transfer dependence of the form factors was discussed and rejected. It was also observed that the charged-particle momentum spectrum is effectively independent of the value of $\xi(0)$, for $\xi(0)$ between zero and 1.0. Thus, any incorrectness of the branching ratio measurements is not likely to be due to assumptions of the ξ parameter in the various data analyses.

Examination of Fig. 1 shows that our result of $\Gamma(K_{\mu 2})/\Gamma(K_{\pi 2}) = 3.28 \pm 0.18$ is in agreement with previous results in the region of 3.0,[4, 11] but is in conflict with the results lying in the region of 2.5.[1, 2, 12] Thus, when establishing a weighted average for these measurements we have excluded the latter, low results. This weighted average is 3.08 ± 0.05, and is in good agreement with both the previous spectrometer spark chamber measurement[11] and this experiment.

ACKNOWLEDGMENT

We thank the staff of the Lawrence Radiation Laboratory for their assistance throughout all phases of the experiment. Most notably we thank R. Fulton, R. Peters, and K. Mirk of the Mechanical Engineering Department, L. Proehl and F. Kirsten of the Nuclear Instrumentation Department, and the operating crew of the Bevatron. We also acknowledge the help of Dr. P. Steinberg during the running of the experiment, and the scanning staff, especially P. Craig and J. Bistirlich, during the analysis phase.

FOOTNOTES AND REFERENCES

*Work done under auspices of the U. S. Atomic Energy Commission.

†Present address: Department of Physics, University of Notre Dame, Notre Dame, Indiana, 46556.

‡Present address: 1478 Ridge Street, Redlands, California.

**Present address: Physics Department, University of California–San Diego, La Jolla, California.

1. G. Alexander, R. H. W. Johnston, and C. O'Ceallaigh, Nuovo Cimento 6, 478 (1957).

2. R. W. Birge, D. H. Perkins, J. R. Peterson, D. H. Stork, and M. N. Whitehead, Nuovo Cimento 4, 834 (1956).

3. S. Taylor, G. Harris, J. Orear, J. Lee, and P. Baumel, Phys. Rev. 114, 359 (1959).

4. B. P. Roe, D. Sinclair, J. L. Brown, D. A. Glaser, J. A. Kadyk, and G. H. Trilling, Phys. Rev. Letters 7, 346 (1961).

5. F. S. Shaklee, G. L. Jensen, B. P. Roe, and D. Sinclair, Phys. Rev. 136B, 1423 (1964).

6. G. Borreani, G. Rinaudo, and A. E. Werbrouck, Phys. Letters 12, 123 (1964).

7. V. Bisi, G. Borreani, R. Cester, A. DeMarco-Trabucco, M. T. Ferrero, C. M. Garelli, A. Marzari-Chiesa, B. Quassiati, G. Rinaudo, M. Vigone, and A. Werbrouck, Nuovo Cimento 35, 768 (1965).

8. A. Callahan and D. Cline, Phys. Rev. Letters 15, 129 (1965).

9. A. C. Callahan, U. Camerini, R. D. Hantman, R. H. March, D. L. Murphree, G. Gidal, G. E. Kalmus, W. M. Powell, C. L. Sandler, R. T. Pu, S. Natali, and M. Villani, Phys. Rev. 150, 1153 (1966).

10. G. H. Trilling, in Proc. Argonne Intern. Conf. on Weak Interactions, Argonne National Laboratory Report ANL-7130, 1965, pp. 115-149.

11. L. B. Auerbach, J. MacG. Dobbs, A. K. Mann, W. K. McFarlane, D. H. White, R. Cester, P. T. Eschstruth, G. K. O'Neill, and D. Yount, Phys. Rev. 155, 1505 (1967).

12. R. L. Beck, A Measurement of the Relative Branching Ratio $(K^+ \rightarrow \mu^+ + \nu)/(K^+ \rightarrow \pi^+ + \pi^0)$ (Ph.D. Thesis), Lawrence Radiation Laboratory Report UCRL-16003, July 28, 1966.

13. Aachen-Bari-CERN-Orsay-Padova-Paris-Valencia-Madrid Collaboration, in Proceedings of the International Conference on Elementary Particles, Heidelberg, Germany, 1967 (North Holland, Amsterdam, 1968).

14. R. Garland, Kosta Tsipis, S. Devons, J. Rosen, D. Tycko, L. G. Pondrom, and S. L. Meyer, Phys. Rev. 167, 1225 (1968).

15. D. R. Botterill, R. M. Brown, A. B. Clegg, I. F. Corbet, G. Culligan, J. McL. Emmerson, R. C. Field, J. Garvey, P. B. Jones, N. Middlemas, D. Newton, T. W. Quirk, G. L. Salmon, P. H. Steinberg, and W. S. C. Williams, Phys. Rev. Letters 21, 766 (1968).

16. K. K. Young, M. J. Longo, and J. A. Helland, Phys. Rev. Letters 18, 806 (1967).

17. D. Cutts, M. Deutsch, R. Stiening, and C. Wiegand, Measurement of the Polarization of the Muon from $K_{\mu 3}$, Phys. Rev. Letters 20, 955-8 (Apr. 22, 1968).

18. L. B. Auerbach, A. K. Mann, W. K. McFarlane, and F. J. Sciulli, Phys. Rev. Letters 19, 464 (1967).

19. B. d'Espagnat and M. K. Gaillard, Phys. Letters 25B, 346 (1967).

20. M. E. Zeller, Measurement of the Branching Ratios of the Decay of the K^+ Meson (Ph. D Thesis); UCLA Report 34P106-26, 1968 (unpublished).

21. P. Dennery and H. Primakoff, Phys. Rev. 131, 1334 (1963).

22. W. J. Willis, Rapporteur talk, in Proceedings of the International Conference on Elementary Particles, Heidelberg, Germany, 1967 (North-Holland, Amsterdam, 1968).

23. L. Okun, Ann. Rev. Nucl. Sci. 9, 61 (1959).

24. N. Cabibbo, Weak Interactions, in Proceedings of the XIII International Conference on High Energy Physics (University of California Press, Berkeley, 1967), p. 29.

25. The use of $\lambda_+ = 0.023$ is a slight departure from the usual analysis for which λ_+ is taken as 0.0 (Refs. 1-12). The difference in the determination of $\xi(q^2)$ from the previous evaluations is a reduction of ξ by approximately 5%. The values of $\xi(q^2)$ in Fig. 2 have all been evaluated with $\lambda_+ = 0.023$ and the respective experimentally determined branching ratios.

26. J. Borggreen, B. Elbek, and L. Perch Nielsen, Nucl. Instr. Methods 24, 1 (1963).

27. L. Landau, J. Phys. 8[4], 201 (1944).

28. W. Heitler, The Quantum Theory of Radiation, 3rd ed. (Oxford Press, 1954).

29. R. R. Wilson, Phys. Rev. 84, 100 (1951).

30. J. F. Tracy, Phys. Rev. 91, 960 (1953).

31. C. Chedester, P. Isaacs, S. Sachs, and J. Steinberger, Phys. Rev. 82, 958 (1951).

32. Approximately 30% of the final data sample did not have decay-time information. In order to include these events, a subtraction was made from the data to account for the events occurring outside the time gates (Refs. 20, 33).

33. N. T. Dairiki, A Measurement of the K^+ Branching Ratios $K_{\mu 2}^+$, $K_{\pi 2}^+$, K_{e3}^+, $K_{\mu 3}^+$, Lawrence Radiation Laboratory Report UCRL-18245.

34. J. Orear, Notes on Statistics for Physicists, Lawrence Radiation Laboratory Report UCRL-8417, 1957.

35. A. H. Rosenfeld, A. Barbaro-Galtieri, J. Kirz, W. J. Podolsky, M. Ross, W. J. Willis, and C. G. Wohl, Lawrence Radiation Laboratory Report UCRL-8030 (rev.) 1966.

Table I. Results of previous measurements (branching ratios, in %).

Ref.	Experiment	$K^+ \to \mu^+ + \nu$ $K_{\mu 2}$	$K^+ \to \pi^+ + \pi^0$ $K_{\pi 2}$	$K^+ \to \mu^+ + \pi^0 + \nu$ $K_{\mu 3}$	$K^+ \to e^+ + \pi^0 + \nu$ K_{e3}	$K_{\mu 3}/K_{e3}$	$K^+ \to 2\pi^+ + \pi^-$ τ^+	$K^+ \to \pi^+ + 2\pi^0$ $\tau^{+\prime}$	Method
1	Alexander et al. '57	56.9 ±2.6	23.2 ±2.2	5.9 ±1.3	5.1 ±1.3	1.16 ±0.39	6.8±0.4	2.2±0.4	Emulsion
2	Birge et al. '59	58.5 ±3.0	27.7 ±2.7	2.8 ±1.0	3.2 ±1.3	0.88 ±0.47	5.6±0.4	2.1±0.5	Emulsion
3	Taylor '59			2.8 ±0.4			5.2±0.3	1.5±0.2	Emulsion
4	Roe et al. '61	64.2 ±1.3	18.6 ±0.9	4.8 ±0.6	5.0 ±0.5	0.96 ±0.15	5.7±0.2	1.7±0.2	Xe BC
5	Shaklee et al. '64	63.0 ±0.8	22.4 ±0.8	3.8 ±0.5	4.7 ±0.3	0.63 ±0.10	5.1±0.2	1.8±0.2	Xe BC
6	Borreani '64				5.12±0.36				H_2 BC
7	Bisi '65			3.45±0.56					H_2 BC
8	Callahan et al. '65		21.0 ±0.56						Propane freon BC
9	Callahan et al. '66		21.0 ±0.9	2.77±0.19	3.94±0.21	0.703±0.056			Freon BC
10	Trilling '65	63.5 ±0.7	21.6 ±0.6	3.17±0.35	4.49±0.25	0.706±0.087			(Summary)
11	Auerbach et al. '67	63.34±0.44	20.61±0.32	3.81±0.26	4.96±0.13	0.767±0.052			Spectrometer and spark chambers
12	Beck '66		$K_{\mu 2}/K_{\pi 2}$ = 2.31±0.24						Spectrometer
13	ABC OPPVM Collab. '67					0.62 ±0.047			Bubble chamber
14	Garland et al. '67			3.5 ±0.3	4.4 ±0.4	0.80 ±0.10			Spectrometer
15	Botterill et al. '68			3.29±0.11	4.94±0.11	0.667±0.017			Spectrometer

Table II. Summary of uncertainties and errors (%).

	Sources of Errors			
	$K_{\mu 2}$	$K_{\pi 2}$	$K_{\mu 3}$	K_{e3}
Statistical fluctuation: Data	±0.8	±3.0	±6.3	±5.8
Statistical fluctuation: Monte Carlo	±1.0	±1.5	±3.5	±3.5
Tracking program[a]	±3.0	±3.0	±3.0	±3.0
Location of pieces of apparatus[a]	0.0	0.0	±1.0	±1.0
Pion nuclear absorption cross sections[a]		±1.4		
Energy-loss calculations	±0.8	±2.5	±0.8	±1.0
Electron scattering				±3.0

a. These errors do not affect $\Gamma(K_{\mu 3})/\Gamma(K_{e3})$

Table III. Range-momentum arrays.

ΔR (g/cm^{2}Cu)	20.0	120-139	140-159	160-179	180-189	190-235
Range-momentum array: Numbers of events (data minus background)						
			P (MeV/c)			
	5.0	106.2±10.9	134.5±12.5	177.1±18.2	51.5±13.9	
	-6.0	26.7± 5.7	252.3±17.9	448.4±49.5	99.4±59.0	15208.0±154.0
	-20.0			1002.0±33.6		
Range-momentum array: Monte Carlo (arbitrary normalization)						
			$K_{\mu 2}$			
				0.13	0.56	
			0.13	0.52	1.26	556.44
				0.82		
			$K_{\pi 2}$			
			1.28	10.15	5.57	
		0.57	13.18	37.47	15.26	3.87
				117.58		
			$K_{\mu 3}$			
		7.07	5.43	3.03	0.55	
		13.93	72.18	49.72	4.95	0.95
				1.16		
			K_{e3}			
		46.76	68.62	39.05	7.48	
		4.68	12.81	10.96	1.34	3.48
				1.71		
Monte Carlo results scaled by branching ratios and summed:						
		95.9	144.0	163.7	75.9	
		33.8	242.6	418.3	170.7	15204.5
				1002.5		

Figure Captions

Fig. 1. Branching ratio of previous measurements.

Fig. 2. Comparison of $\xi(q^2)$ by branching ratio and polarization.

Fig. 3. Plan view of K^+ beam arrangement.

Fig. 4. Schematic drawing of Elbek spectrometer and detection apparatus (the K^+'s enter the scintillator target in a direction out of the plane of the paper).

Fig. 5. Focal plane wire chamber efficiency as a function of momentum.

Fig. 6. Comparison of data and Monte Carlo calculations.

I. Distribution of penetration into the exit chamber of muons from $K_{\mu 2}$.
II. Deviation of actual spark location in the exit chamber from projected positions.
III. Initial spatial distribution of events.
IV. Initial angular distribution of events.

Fig. 7. Momentum spectrum as seen at the focal plane (solid line is data; dashed line is calculated histogram).

Fig. 8. Data scatterplot.

Fig. 9. Distributions with gates.

I. Initial spatial distribution.
II. χ_x^2 distribution.
III. Ratio of events below 190 MeV/c to events above vs decay time.

Fig. 10. Scatterplot of background calculation.

Fig. 11. Scatterplot of $K_{\mu 2}$ Monte Carlo calculation.

Fig. 12. Scatterplot of $K_{\pi 2}$ Monte Carlo calculation.

Fig. 13. Scatterplot of $K_{\mu 3}$ Monte Carlo calculation.

Fig. 14. Scatterplot of K_{e3} Monte Carlo calculation.

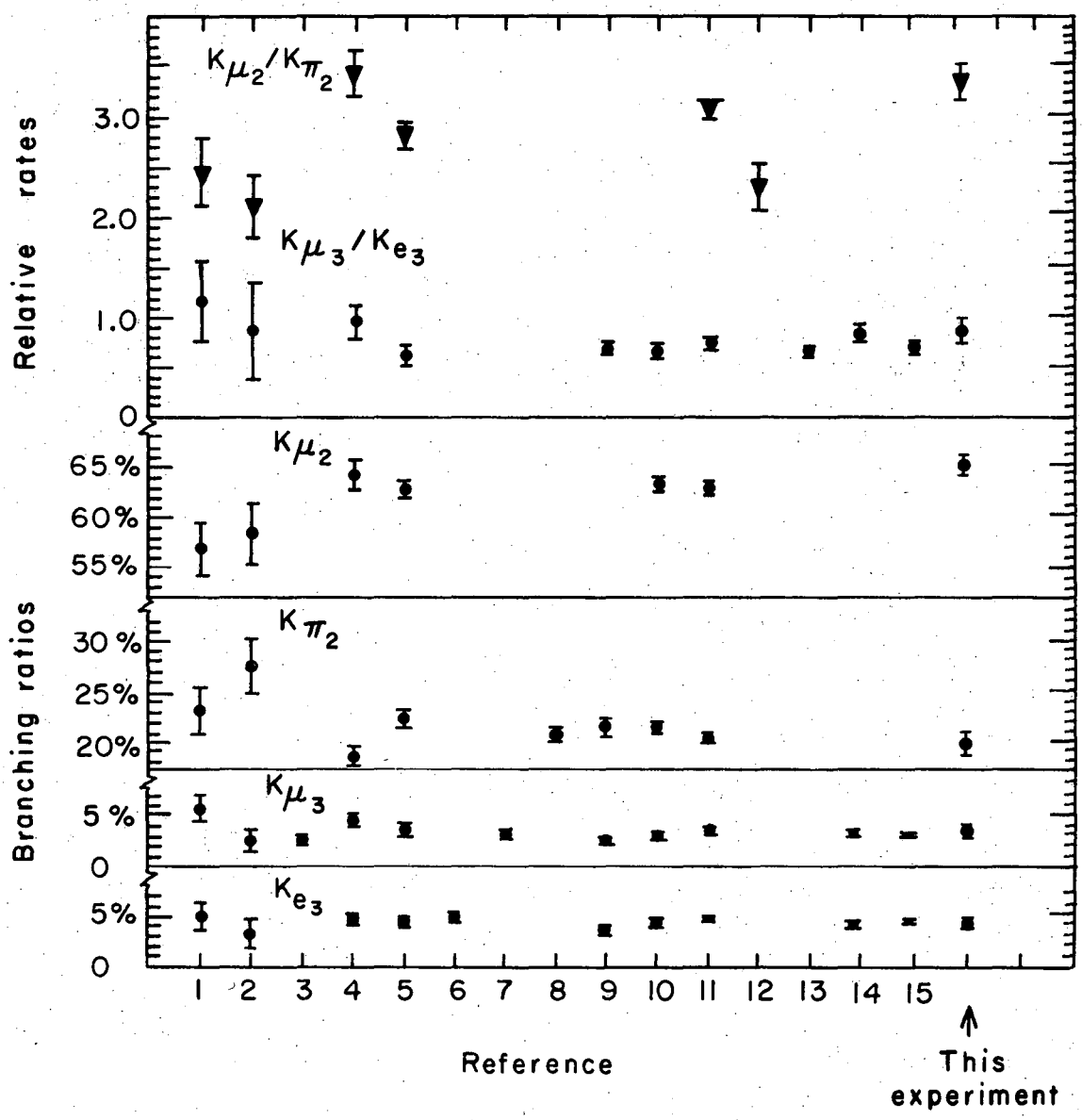

XBL 6810-6012

Fig. 1

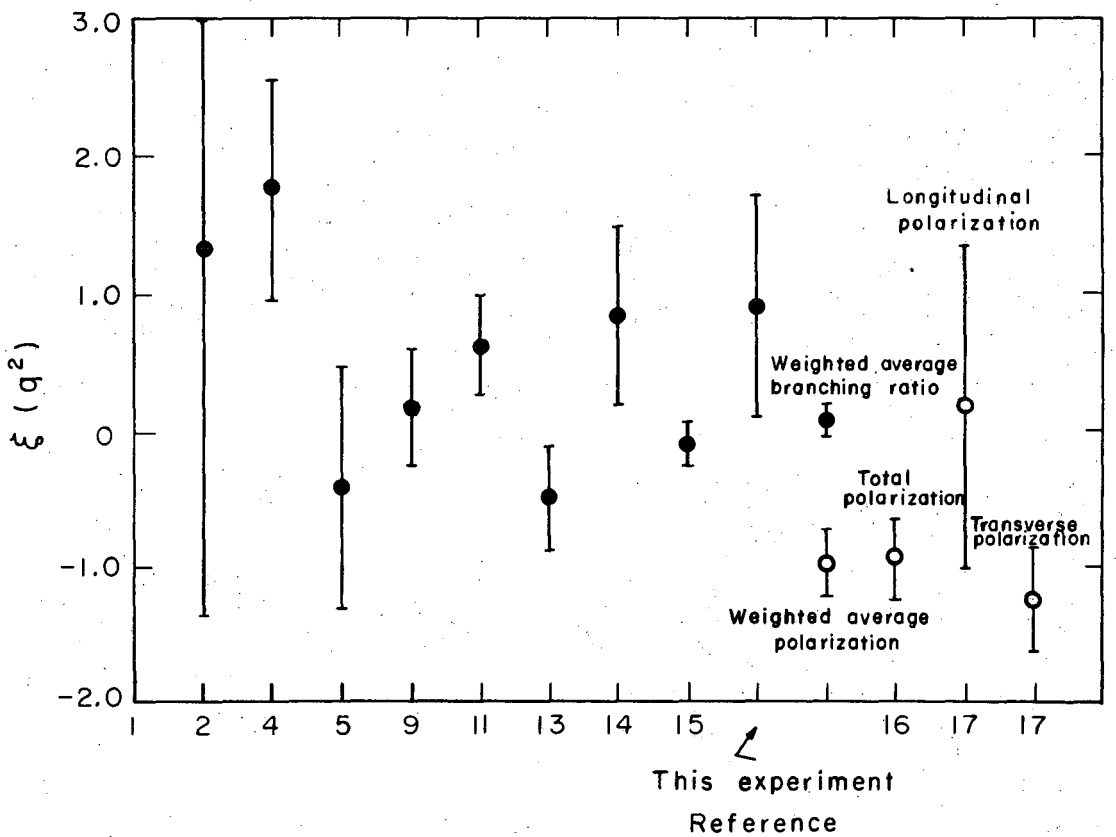

XBL6810-6902

Fig. 2

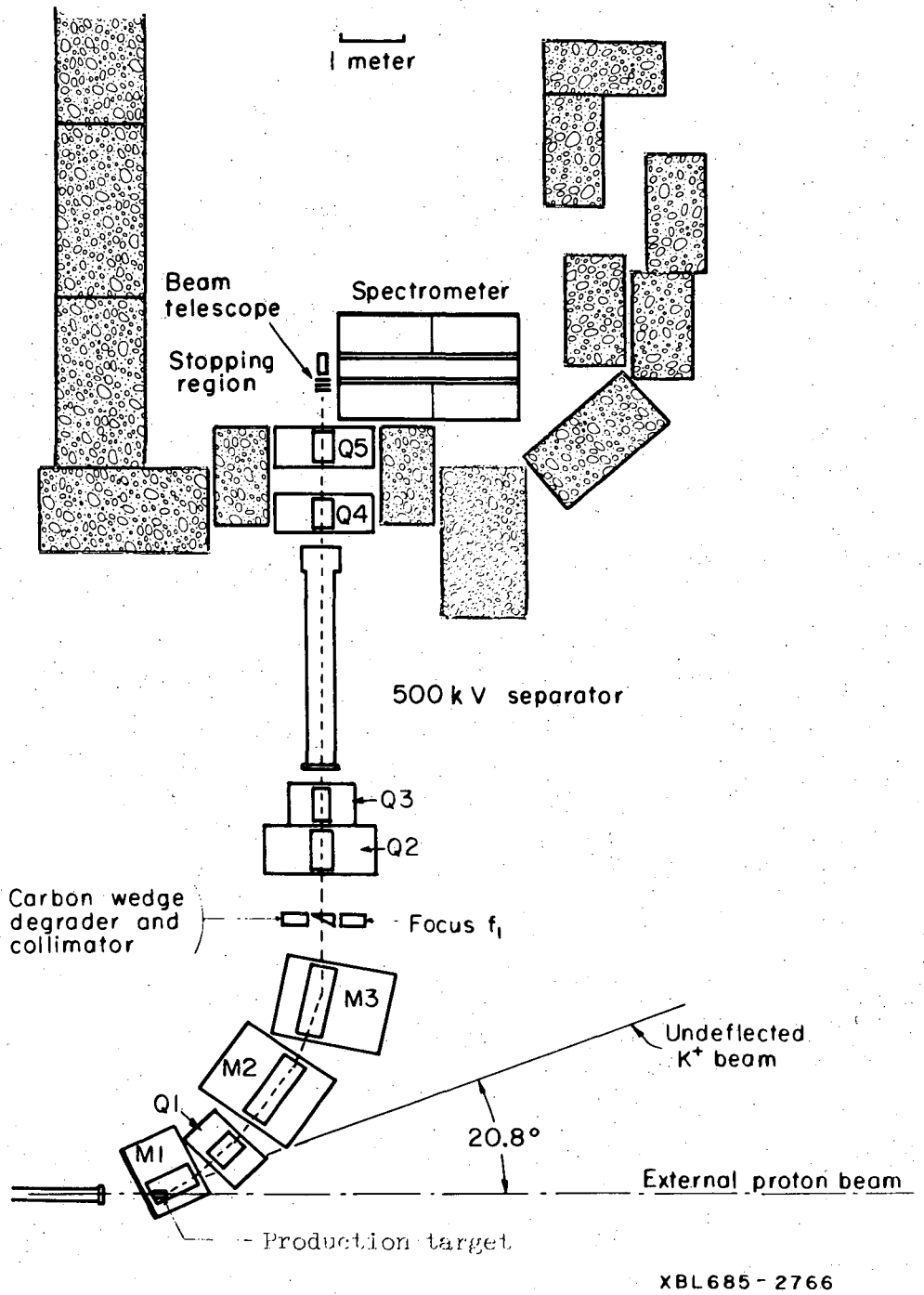
1 meter
Beam telescope
Spectrometer
Stopping region
Q5
Q4
500 k V separator
Q3
Q2
Carbon wedge degrader and collimator
Focus f_1
M3
M2
Q1
M1
Undeflected K^+ beam
20.8°
External proton beam
Production target
XBL685-2766

Fig. 3

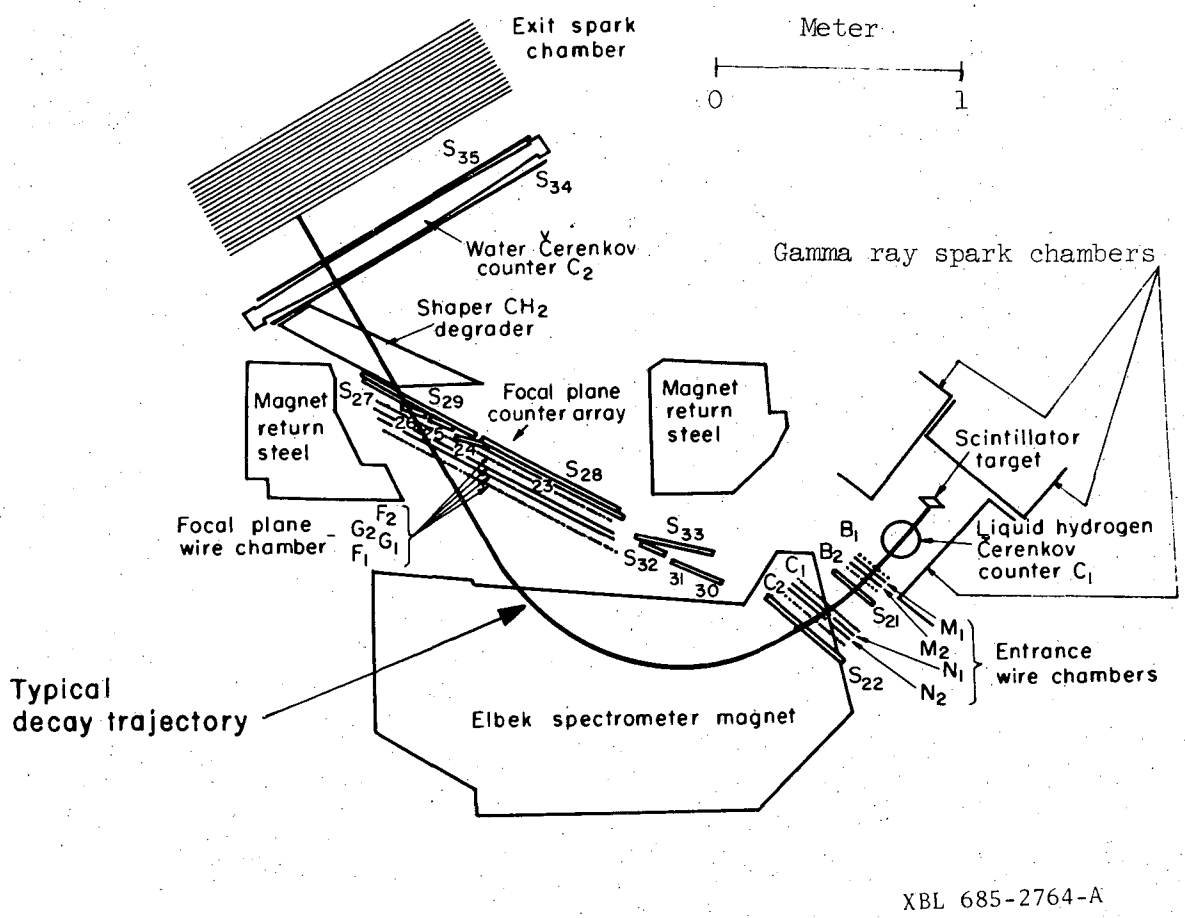
Exit spark chamber
Meter
0
1
S35
S34
Water Čerenkov counter C2
Gamma ray spark chambers
Shaper CH2 degrader
Magnet return steel
S27
S29
Focal plane counter array
Magnet return steel
Scintillator target
S28
Focal plane wire chamber
F2
G2
G1
F1
S33
S32
31
30
B1
B2
Liquid hydrogen Čerenkov counter C1
C1
C2
S21
M1
M2
N1
N2
S22
Entrance wire chambers
Typical decay trajectory
Elbek spectrometer magnet
XBL 685-2764-A

Fig. 4

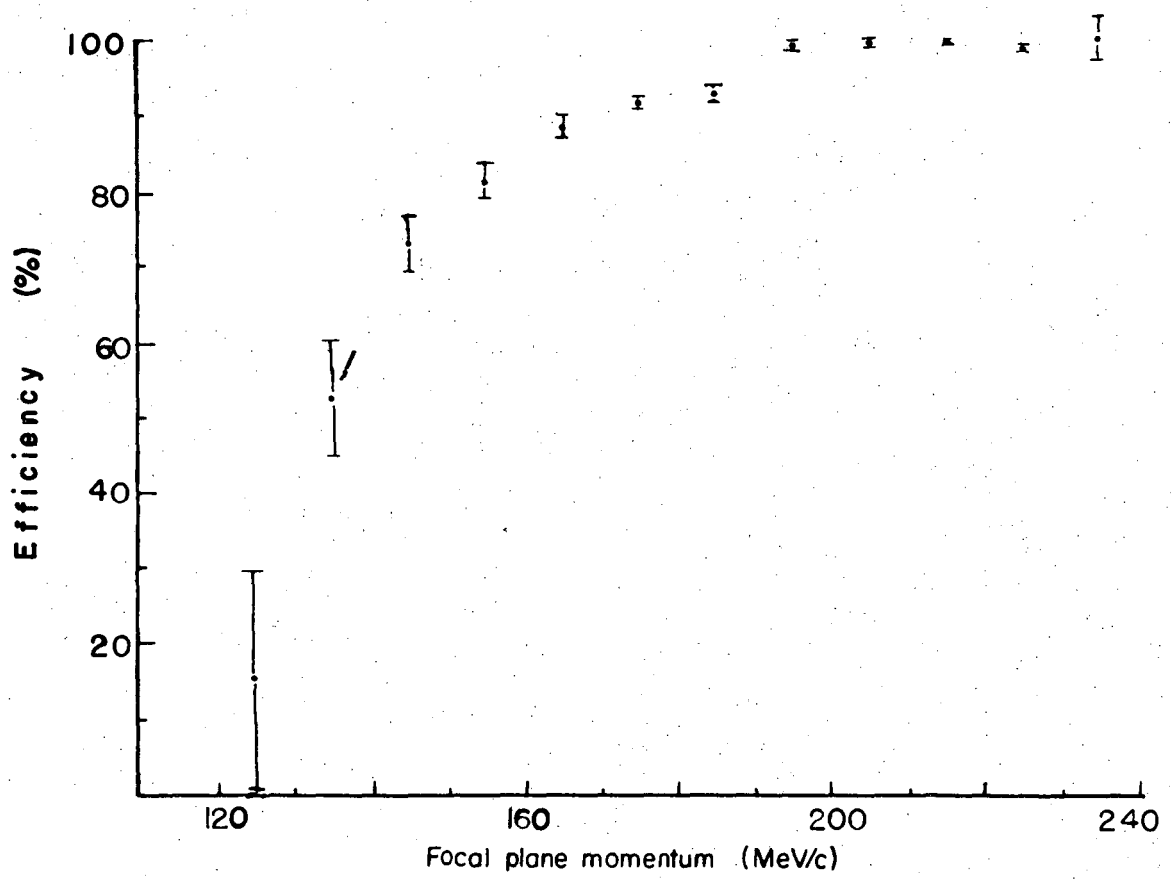

XBL 685-874

Fig. 5

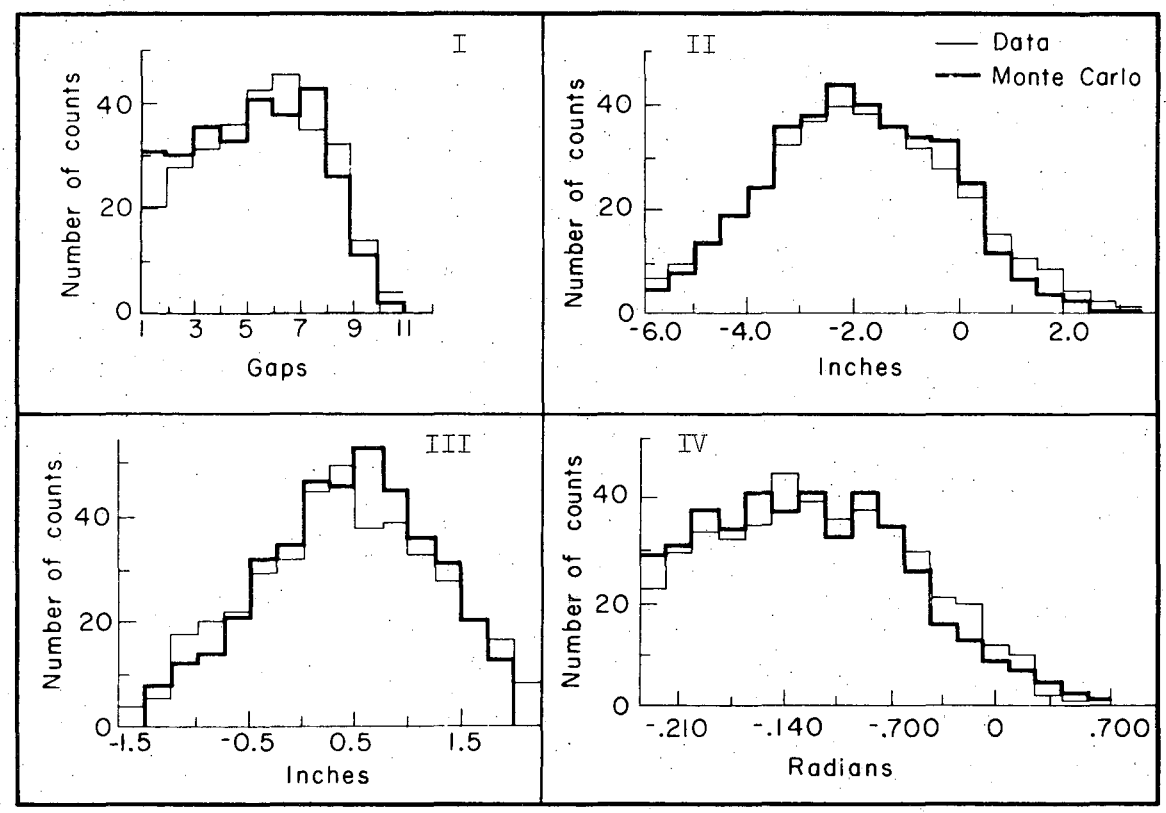

XBL688-3546

Fig. 6

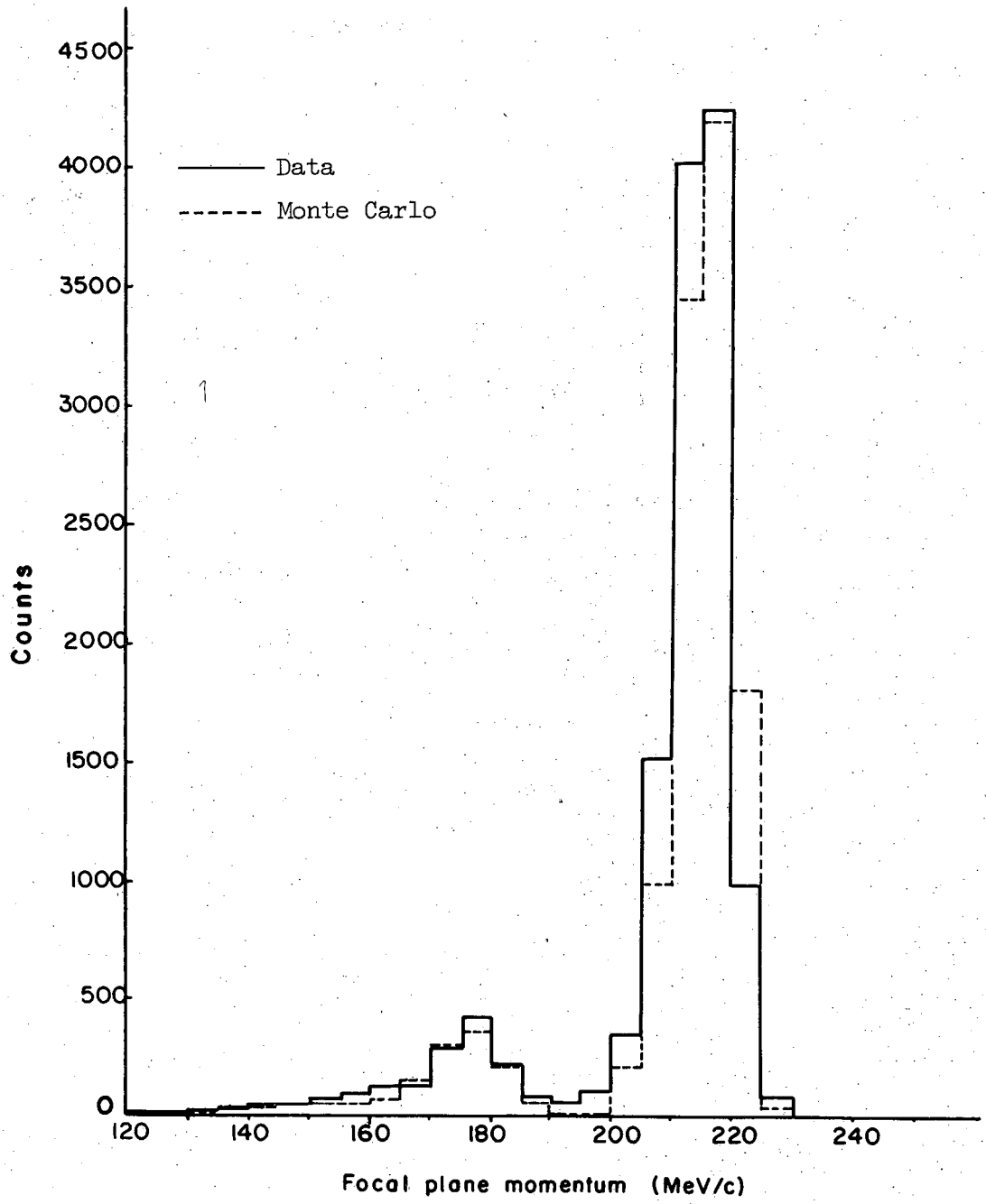

XBL 685-871

Fig. 7

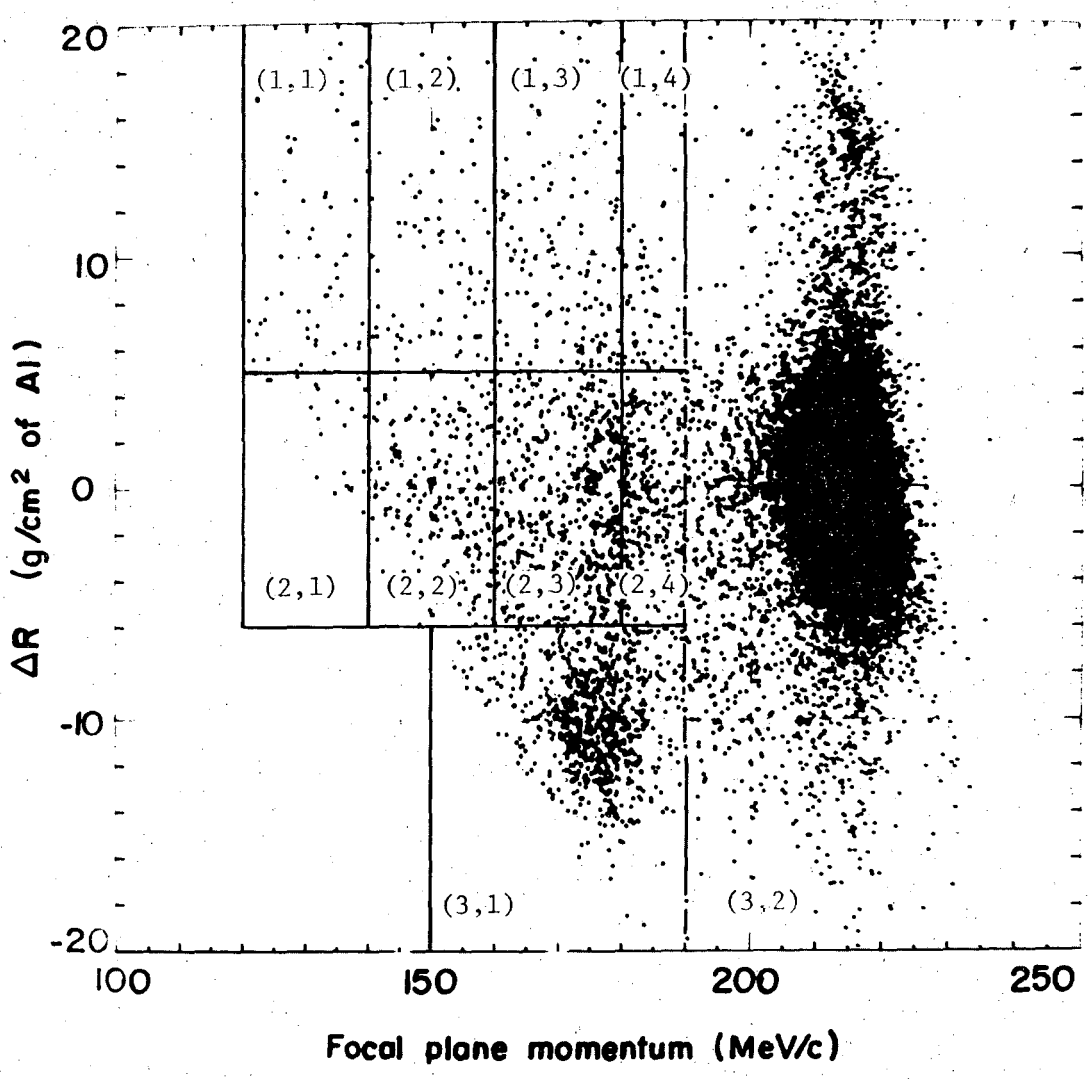

XBB 684-2002

Fig. 8

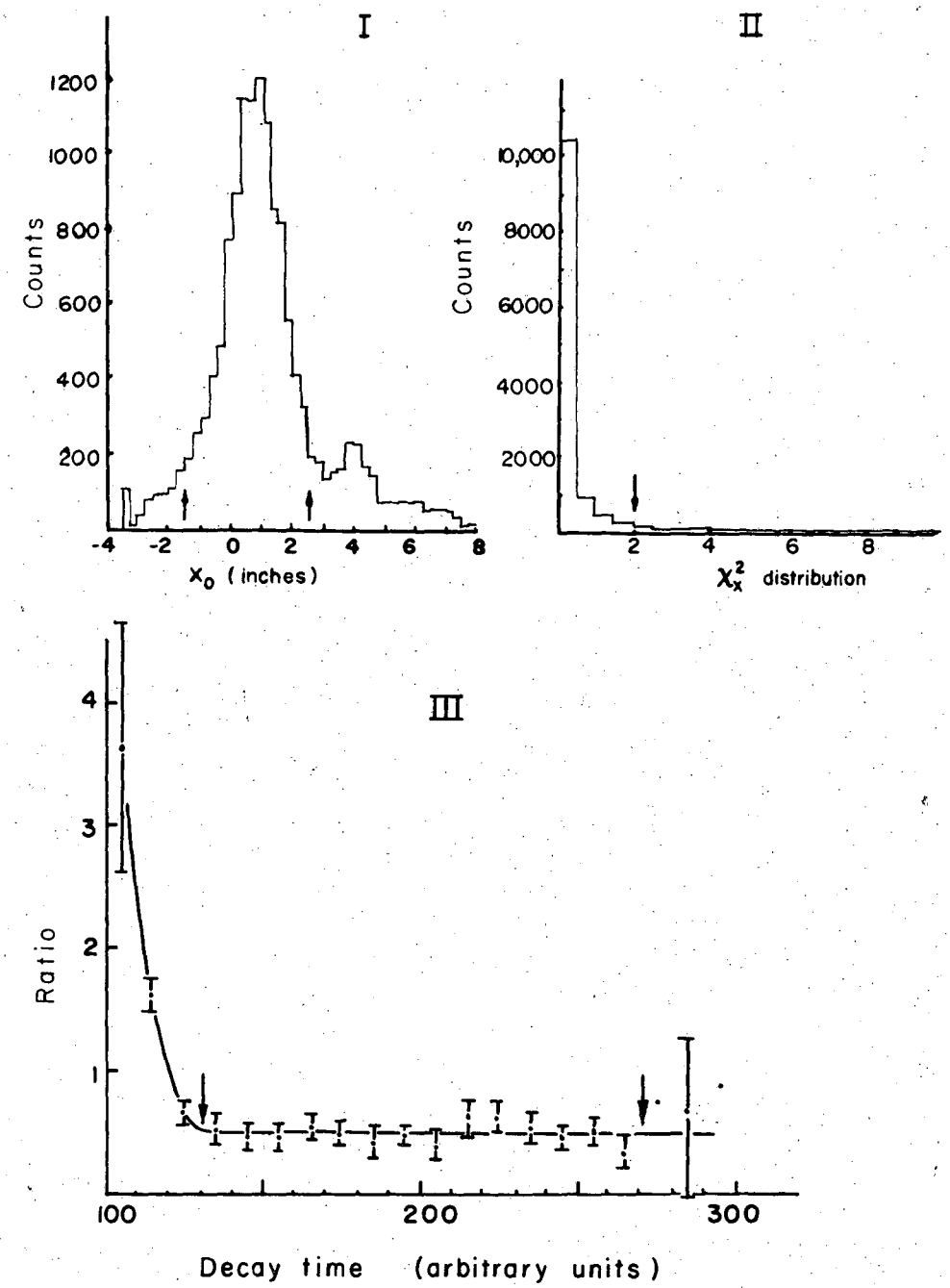

XBL 685-864-A

Fig. 9

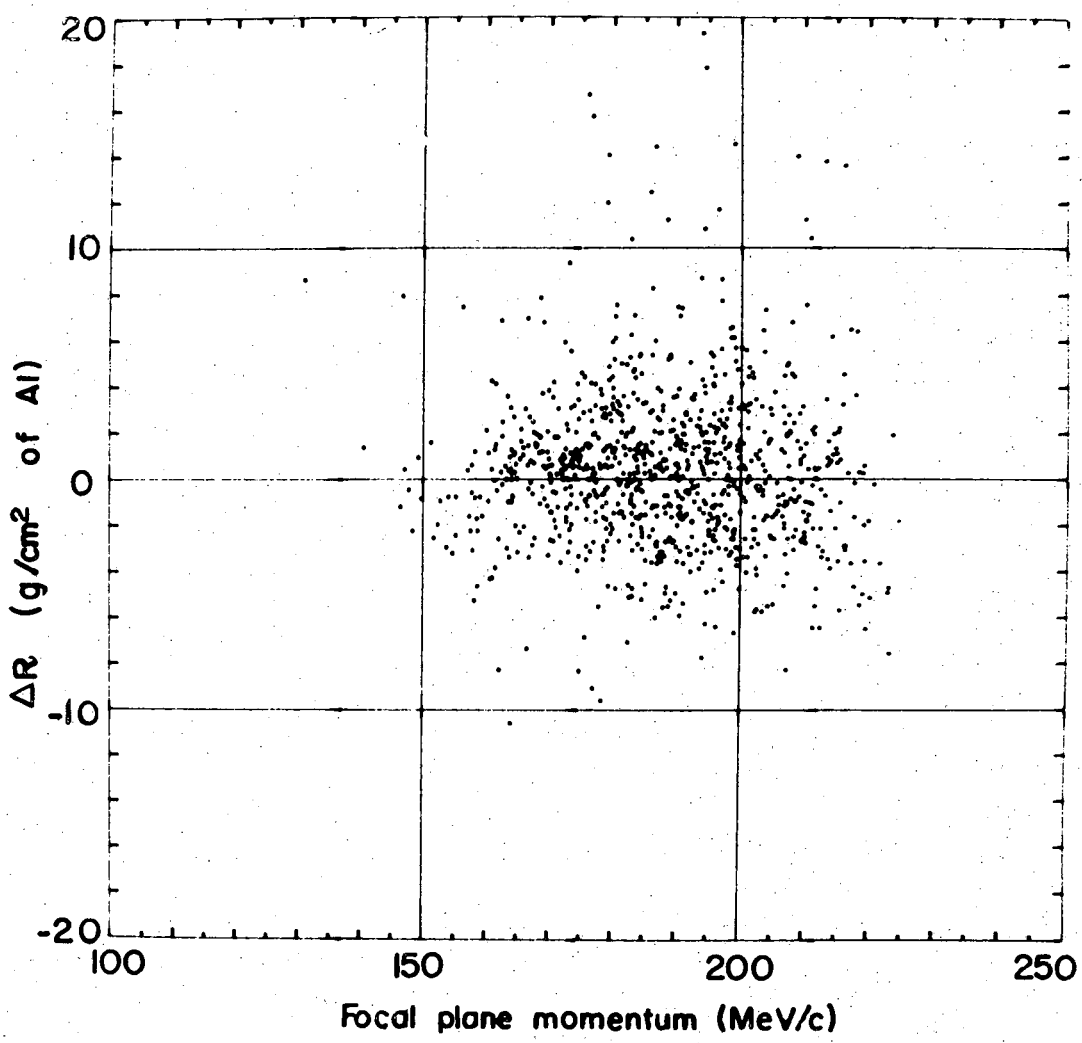

XBB 684-1996

Fig. 10

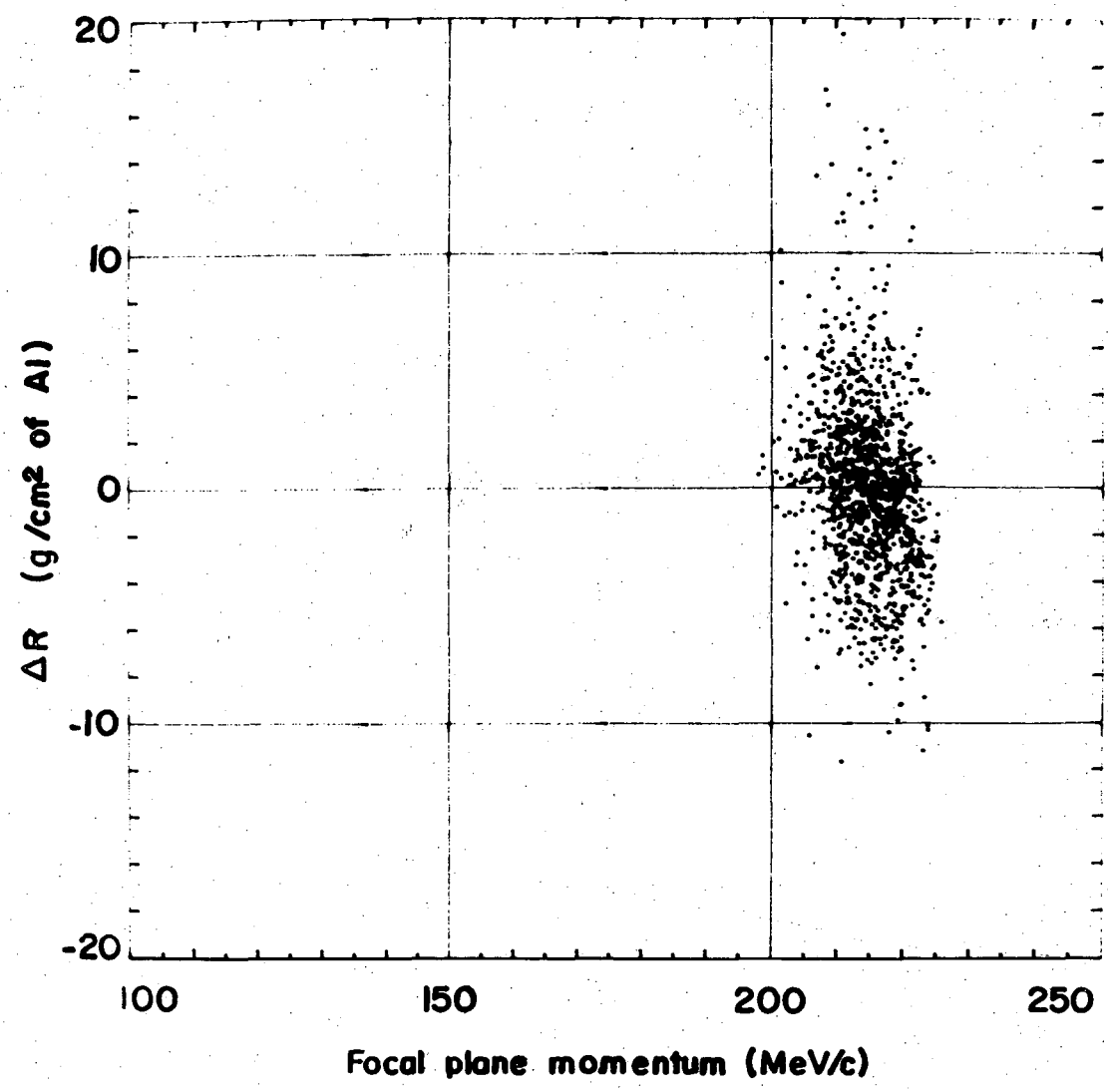

XBB 684-2000

Fig. 11

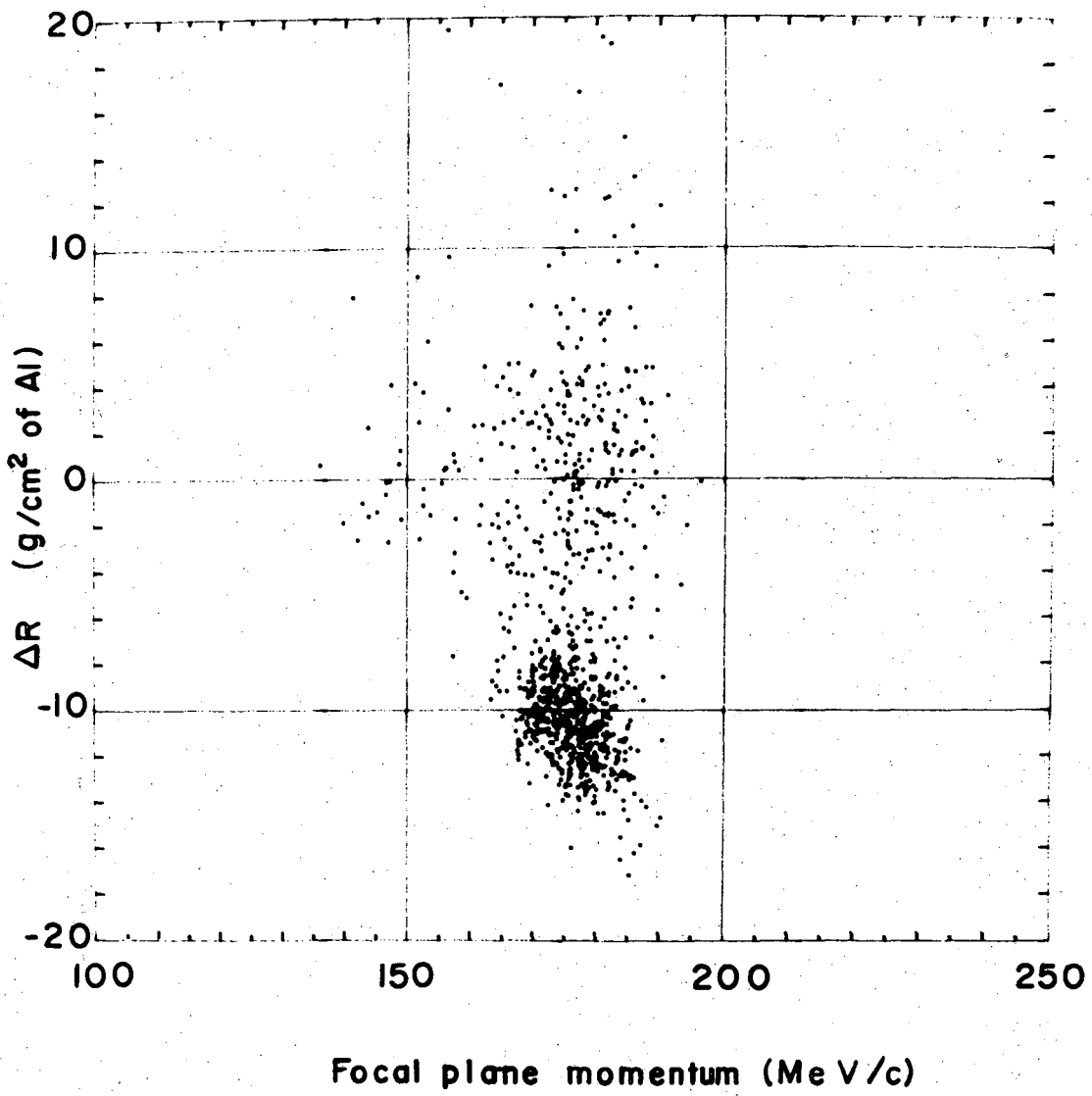

XBB 684-2003

Fig. 12

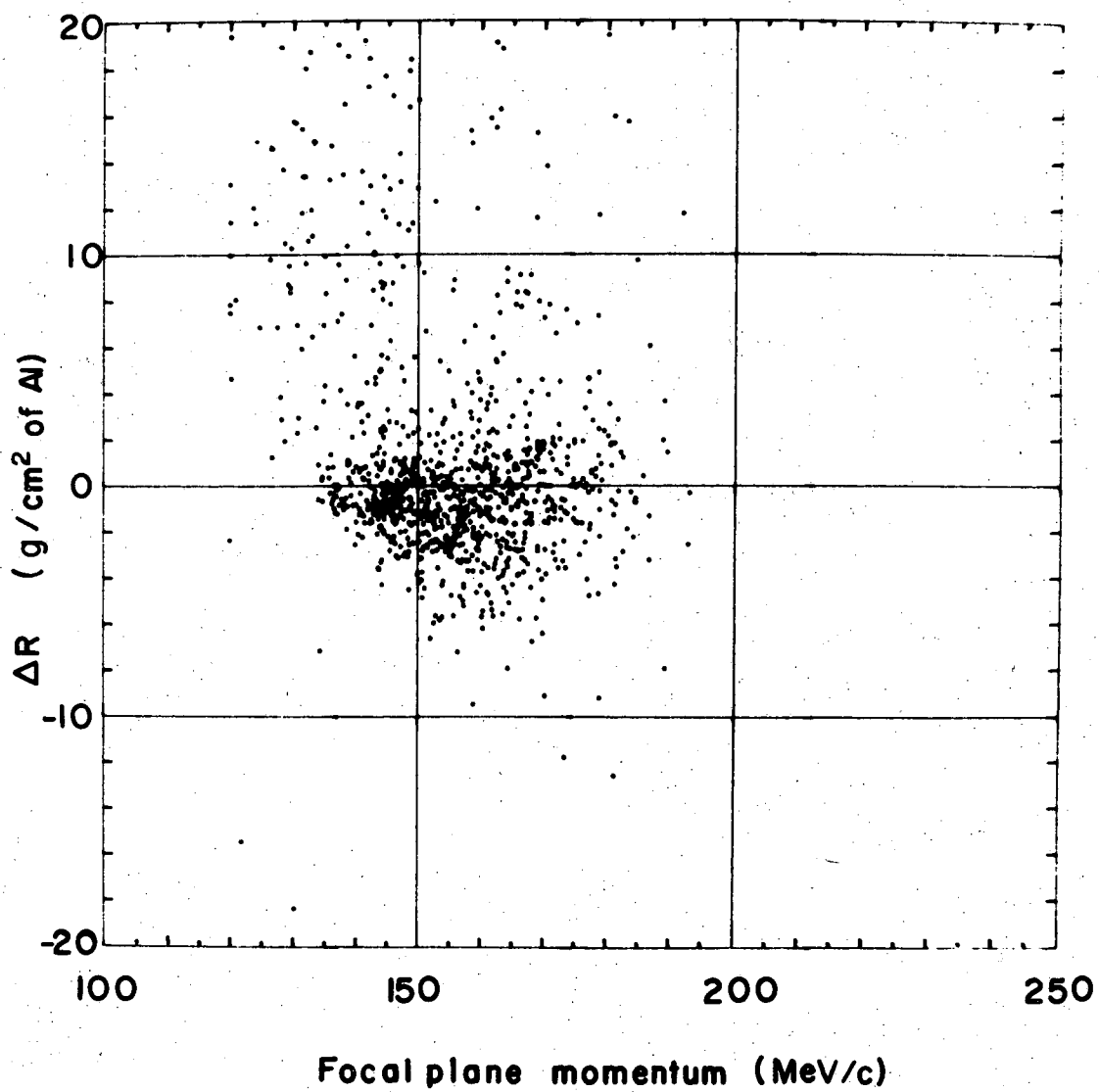

XBB 684-1997

Fig. 13

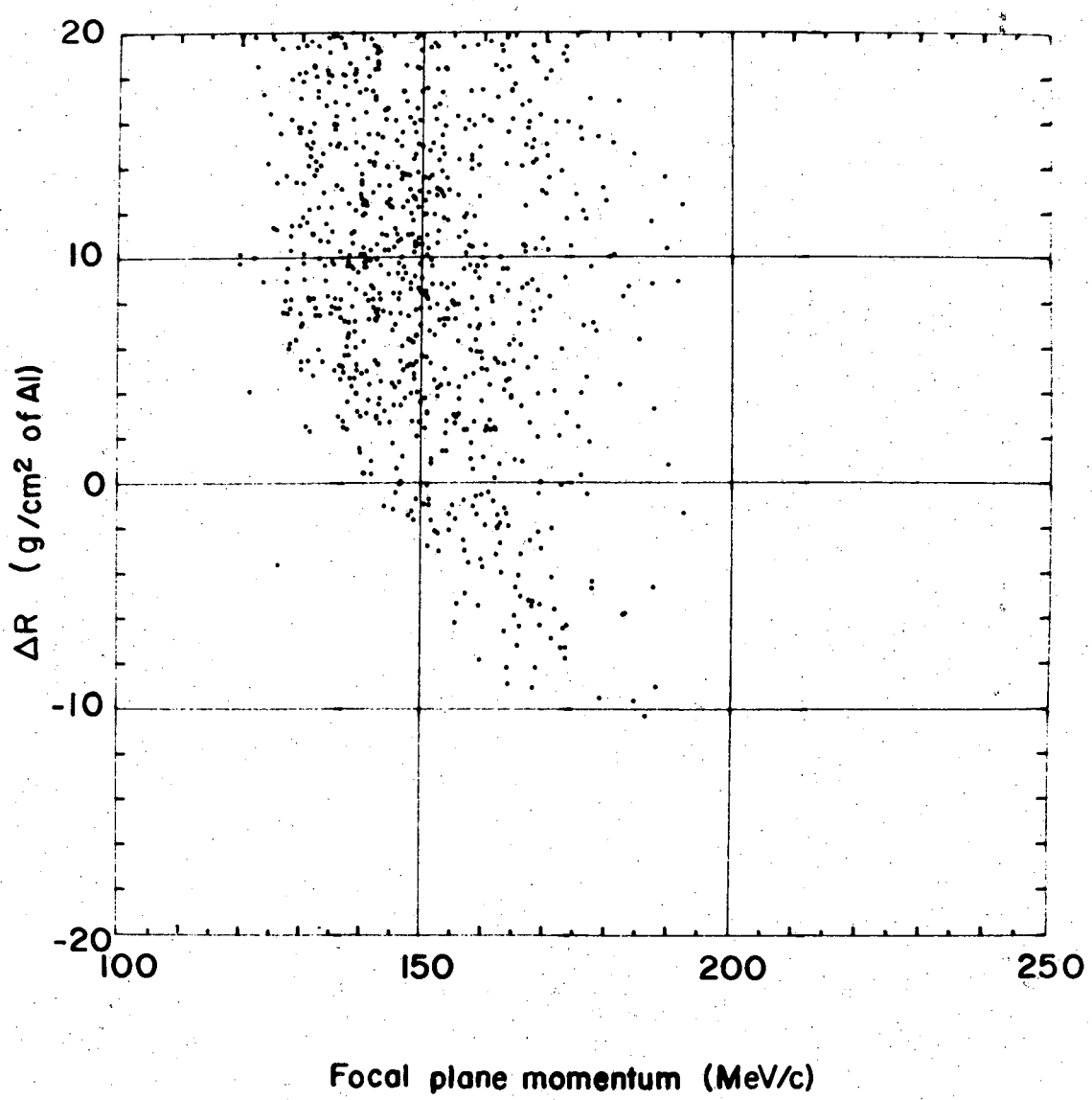

XBB 684-2001

Fig. 14

This report was prepared as an account of Government sponsored work. Neither the United States, nor the Commission, nor any person acting on behalf of the Commission:

A. Makes any warranty or representation, expressed or implied, with respect to the accuracy, completeness, or usefulness of the information contained in this report, or that the use of any information, apparatus, method, or process disclosed in this report may not infringe privately owned rights; or

B. Assumes any liabilities with respect to the use of, or for damages resulting from the use of any information, apparatus, method, or process disclosed in this report.

As used in the above, "person acting on behalf of the Commission" includes any employee or contractor of the Commission, or employee of such contractor, to the extent that such employee or contractor of the Commission, or employee of such contractor prepares, disseminates, or provides access to, any information pursuant to his employment or contract with the Commission, or his employment with such contractor.